Analysis of Filter banks for Multi-carrier communications

Ish Kumar Jain, Zhaoxin Hu

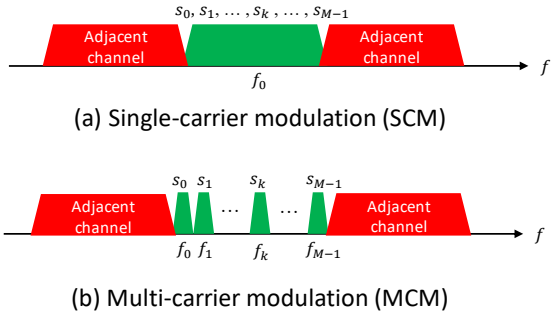

Figure 1: Single carrier vs multi carrier modulation

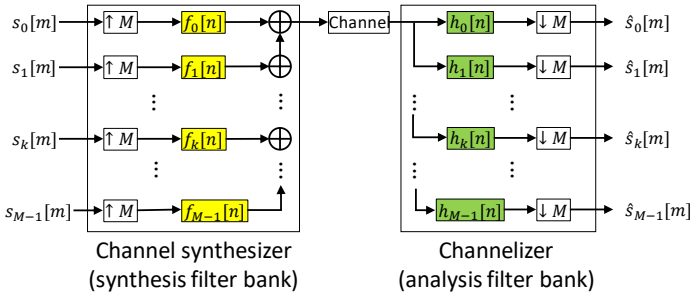

Figure 2: Transmultiplexer (TMux) design

***Abstract*—Multi-carrier modulation with Orthogonal Frequency Division Multiplexing (OFDM) is being used in 4G cellular system and it provides higher data rates compared to previous single-carrier systems. However, OFDM suffers from higher side lobe leakage which limits the spectral efficiency. Various filter banks based on DFT and DCT modulation have been studied to solve this limitation. In this report, we compare the performance of these filter banks and analyse various design tradeoffs. These filter banks generally have higher complexity compared to OFDM, but have better spectral efficiency which is required for many applications such as cognitive radios and OFDMA based multiple access system.**

I. Introduction

OFDM is considered in fourth generation (4G) of cellular network standards because of high data rates and better spectrum usage. Traditional single-carrier waveforms (See Figure 1) limits the signal bandwidth (and thus data rates) in a frequency selective channel (multi-path rich channel) or requires complex receiver (e.g. Rake receiver) to decode the transmitted bits. On the other hand, OFDM uses multiple subcarriers which divides the frequency selective channel into a set of frequency flat channel that is experienced by the signal loaded at each subcarriers. OFDM reduces the receiver complexity by using fast FFT based processing and a simple channel equalization procedure. In addition, OFDM uses a cyclic prefix as a guard band between each symbol in time domain to recover from the impact of multi-path rich fading channel. Overall, the time-domain OFDM symbol is multiplied by a rectangular window (including the cyclic prefix) for the ease of processing and to reduce hardware complexity. The impact of rectangular window in time domain is a sinc spreading in frequency domain at each subcarriers. Even though the DFT based OFDM subcarriers are orthogonal to each other, the unwarrented side lobes due to wide sinc waveform causes spectrum leakage to the adjacent channel in frequency domain. A quick fix used in OFDM based 4G cellular system (LTE or long term evaluation) is to use a guard band in frequency domain, which critically reduces the spectral efficiency.

Several methods have been proposed in literature to improve the spectral efficiency of OFDM based on more complex filter bank (FB) architectures. DFT based FB (popularly known as filter bank for multi-carrier or FBMC) and DCT-based FB (cosine modulated filter bank or CMFB) are the most common examples that are widely explored in last few decades. Both of these methods designs a prototype filter which has some unique properties that it is nearly localized in time as well as in frequency. This protopype filter is then upconverted in frequency domain by modulating through exponential functions (DFT-based) or real cosine functions (DCT-based). The filter bank architecture that is used for the filtering and multiplexing is called a Transmultiplexer (TMux). A TMux is essentially a filter bank with synthesizer first followed by a channelizer as shown in Figure 2.

In this project, we explore the design choices for various prototype filters and analyse the performance tradeoffs. We first study the perfect reconstruction (PR) conditions for both DFT and DCT based TMux design and find ways to achieve that. Our analysis verified that the PR conditions for DFT based TMux is hard to achieve. It requires one of the sysnthesis or analysis filter to be IIR, however, practical system demands FIR filters. Thus, PR cannot be satisfied. The design principle in this case is to design near-PR filters which minimizes the sideband leakage. The special case of FBMC is OFDM where the analysis and synthesis filters are rectangular window. It satisfies PR, however, at the expense of higher side-lobe leakage and higher peak-to-average power ratio (PAPR). On the other hand, CMFB achieves both PR and low side-lobe leakage, but has higher PAPR. Both, OFDM and CMFB has fast implementation available on hardware. However, OFDM is picked for 4G communication system because it works well for multi-path rich fading channel with simple equalization.

We did extensive analysis to compare the three approaches

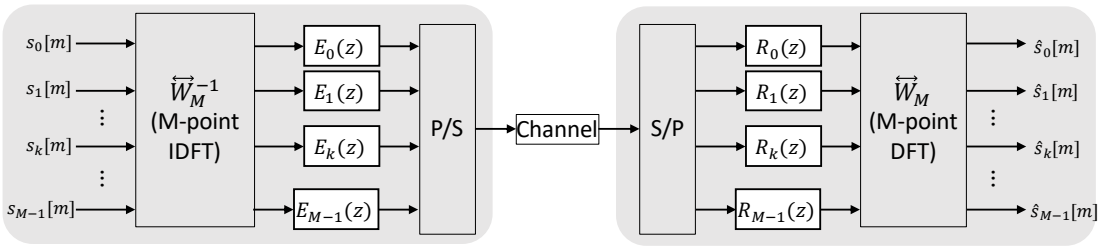

Figure 3: FBMC TMux in polyphase form.

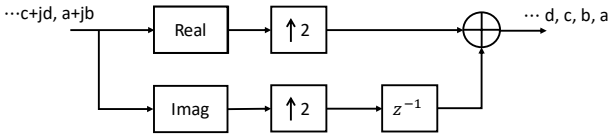

Figure 4: OQAM processing: From complex to real symbols

in terms of power spectral density (PSD) to understand the side lobe leakage and bit error rate (BER) to understand the near perfect reconstruction under additive white Gaussian noise (AWGN) channel. For FBMC, we used PHYDYAS filter to obtain the results. For CMFB, we compare different filters obtained from Kaiser or Chebyshev windows and reveal various performance tradeoffs. In conclusion, this work provides a good survey tutorial on filter banks based approaches for multi-carrier communication and highlights various design tradeoffs.

II. FBMC: DFT BASED TMUX

In DFT based TMux, the analysis filters $H_k(z)$ are all modulation $H_k(z) = H_0(zW^k)$ of a low pass prototype filter, where $W = e^{j2\pi/M}$. The synthesis filters are defined similarly. We can implement the synthesis and analysis filter banks in polyphase form as shown in Figure 3:

$$H_p(z) = [\text{DFT}](diag)(R_0(z), R_1(z), \ldots, R_{M-1}(z)), \quad (1)$$

where $R_k(z)$ for $k = 1, \ldots, M$ are the polyphase components of the prototype filter $H_0(z)$. Recall that the TMux is a synthesizer at the transmitter and a channelizer at the receiver node. The PR conditions for DFT based Filter bank is obtained as

$$E_k(z)R_k(z) = z^{-1} \quad \forall k. \quad (2)$$

For DFT based TMux, we have the same PR condition except that the TMux synthesizer filters need to have a delay z^{-1} in addition to PR condition in (2). This delay term can be incorporated in the wireless channel [1]. Note that to satisfy the PR condition in (2), we have $R_k(z) = z^{-L}E_k^{-1}(z)$, which is IIR rather than FIR. In practice the FIR filters are used because they are easy to design and implement. Thus the perfect reconstruction is not possible except for a special case when $E_k(z) = R_k(z) = 1$ for all k, which is nothing but an OFDM system.

The prototype filters in FBMC is to designed to satisfy near PR (NPR) condition and not exact PR. It is because the reconstruction error is generally low compared to the imparements due to wireless channel and NPR filters can be designed to have very low side band attenuation. A standard design principle is based on Frequency Sampling Technique [2] which is used by PHYDYAS project [3] in 2009. The filter is designed in the following form. The details are omitted for brevity.

$$p[m] = P[0] + 2\sum_{k=1}^{K-1}(-1)^k P[k]\cos\left(\frac{2\pi k}{KM}(m+1)\right) \quad (3)$$

where $m = 0, 1, \ldots, KM-2$, K is overlapping factor ($K > 3$) and the filter length is $L = KM$. Finally, it is important to mention that the communication symbols are complex but the filter need real samples. So we use OQAM processing as shown in Figure 4 to convert complex symbol to real by offsetting imaginary part of symbol. In the next section, we will discuss cosine modulated filter banks which can satisfy PR while at the same time minimising the side-band leakage.

III. CMFB: DCT BASED TMUX

In an M-channel CMFB (Figure 5), the analysis filters ($h_k[n]$) and the synthesis filters ($f_k[n]$) are derived from a prototype filter ($p_0[n]$) via cosine modulation. One particular formulation is shown as follows [4], which will be used in this project.

$$h_k[n] = 2p_0[n]\cos((\frac{\pi}{M}(k+0.5)(n-\frac{1}{2}N) + \theta_k) \quad (4)$$

$$f_k[n] = 2p_0[n]\cos((\frac{\pi}{M}(k+0.5)(n-\frac{1}{2}N) - \theta_k) \quad (5)$$

where

$$\theta_k = (-1)^k\frac{\pi}{4} \quad (6)$$

In this formulation, $p_0[n]$ is of order $N = 2mM - 1$, where m is an integer. It is a lowpass filter with cutoff frequency around $\frac{\pi}{M}$, and is symmetric ($p_0[n] = p_0[N-n]$). $p_0[n]$ is typically not a rectangular window to minimize sidelobes. The CMFB can be implemented very efficiently with DCT matrices, and can be designed to be PR if every pair of $2M$-polyphase components $p_0[n]$ satisfies the power complementary (PC) condition as below [4].

$$G_k(z^{-1})G_k(z) + G_{M+k}(z^{-1})G_{M+k}(z) = 1 \quad (7)$$

where $0 \leq k \leq M-1$, and

$$Z^{-1}\{G_k(z)\} = g_k[n] = p_0[k+2Mn] \quad (8)$$

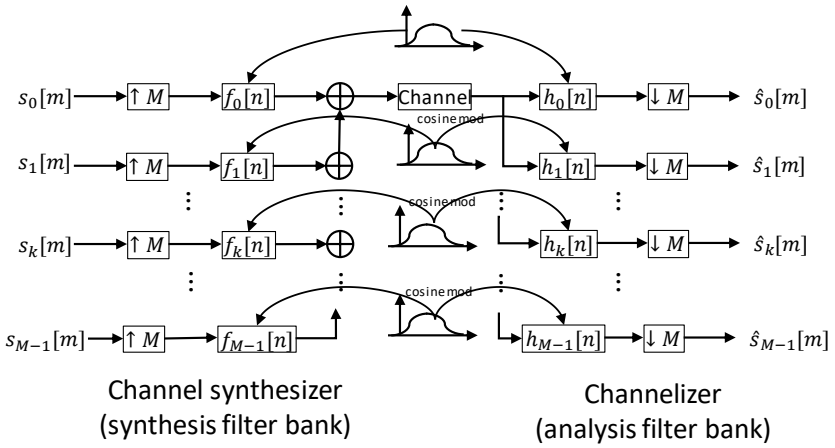

Figure 5: Cosine modulated TMux

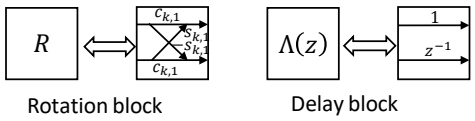

Figure 6: Rotation and delay blocks for filter design.

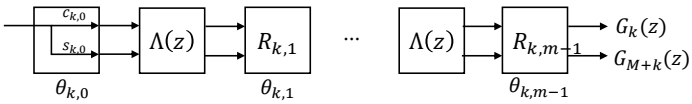

Figure 7: Cosine modulated filter design

is the k^{th} $2M$-polyphase component of $p_0[n]$.

To design prototypes that satisfy PC, an effective approach employs the rotation and delay "building blocks" for orthogonal FB [4] as shown in Figure 6. They are used to design every pair of polyphase components ($G_k(z)$ and $G_{M+k}(z)$). If each polyphase component has m coefficients, m rotation blocks ($R_{k,0}$ through $R_{k,m-1}$ for the k^{th} pair) should be used, with delay blocks inserted in between (Figure 7). Note that the 0^{th} rotation block is different from all other ones in that it does not have cross-channel paths.

To determine $\theta_{k,l}$ of the rotation blocks, one approach is to start with angles that are all equal, and optimize until a good stopband attenuation is reached. However, it is generally difficult for the solver to converge to a good design choice.

A "reverse engineering" approach is adopted instead. In this approach, the prototype filter is designed based on modifying some lowpass filter that almost satisfies PC. Initially, a symmetric lowpass filter ($w[n] = w[N-n]$) that almost satisfies PC is chosen as the design starting point. The order is again $N = 2mM - 1$.

Next, $\theta_{k,l}$ are estimated based on the coefficients of the pair of polyphase component ($w_k[n]$ and $w_{M+k}[n]$, where $0 \le k \le M-1$). The details are explained as follows for the cases where $m = 1$ and $m = 2$. The Appendix illustrates this step with an example.

(1) $m = 1$

The polyphase component pair $W_k(z)$ and $W_{M+k}(z)$ ($0 \le k \le M-1$) are shown below.

$$\begin{bmatrix} W_k(z) \\ W_{M+k}(z) \end{bmatrix} = \begin{bmatrix} w_k[0] \\ w_{M+k}[0] \end{bmatrix} \tag{9}$$

where

$$w_k[n] = w[k + 2Mn] \tag{10}$$

Note that in the building block approach, the coefficients of the pair $G_k(z)$ and $G_{M+k}(z)$ are generated as follows.

$$\begin{bmatrix} G_k(z) \\ G_{M+k}(z) \end{bmatrix} = \begin{bmatrix} c_{k,0} \\ s_{k,0} \end{bmatrix} \tag{11}$$

Comparing (9) and (11), if $w[n]$ exactly satisfies PC, its coefficients $w_k[n]$, after normalization (neglected here for simplicity), are then sines or cosines of some angles, and the angles can be computed as follows with inverse tangents which take two arguments and return an angle in any quadrant (atan2()).

$$\theta_{k,0} = \text{atan2}(w_{M+k}[0], w_k[0]) \tag{12}$$

If $w[n]$ almost but not exactly satisfy PC, (12) can still be used to "fit" a set of angles. These angles are then used to compute a new set of coefficients (with the building block approach), and these coefficients form a PC prototype $p_0[n]$ that "mimics" the frequency response of $w[n]$. In addition, it is found in the Appendix that the less $w[n]$ differs from PC, the better $p_0[n]$ mimics $w[n]$. In the limit where $w[n]$ is exactly PC, $p_0[n] = w[n]$. The following expressions can be used to indicate (at least qualitatively) how much $w[n]$ differs from PC. The larger it is, the more $w[n]$ differs from PC.

$$D_k = |1 - w_{M+k}^2[0] - w_k^2[0]| \tag{13}$$

(2) $m = 2$

The polyphase component pair $W_k(z)$ and $W_{M+k}(z)$ are shown below.

$$\begin{bmatrix} W_k(z) \\ W_{M+k}(z) \end{bmatrix} = \begin{bmatrix} w_k[0] + w_k[1]z^{-1} \\ w_{M+k}[0] + w_{M+k}[1]z^{-1} \end{bmatrix} \tag{14}$$

Similarly, the polyphase component pair $G_k(z)$ and $G_{M+k}(z)$ are generated as follow.

$$\begin{aligned}\begin{bmatrix} G_k(z) \\ G_{M+k}(z) \end{bmatrix} &= \boldsymbol{R}_{k,1}\boldsymbol{\Lambda}(z)\begin{bmatrix} c_{k,0} \\ s_{k,0} \end{bmatrix} \\ &= \begin{bmatrix} c_{k,0}c_{k,1} + s_{k,0}s_{k,1}z^{-1} \\ -c_{k,0}s_{k,1} + s_{k,0}c_{k,1}z^{-1} \end{bmatrix}\end{aligned} \tag{15}$$

In this case, if $w[n]$ exactly satisfies PC, its coefficients $w_k[n]$ are then a product of sines and cosines of some angles, and the angles can be computed as follows.

$$\begin{aligned}\cos\theta_{k,0} - \theta_{k,1} &= c_{k,0}c_{k,1} + s_{k,0}s_{k,1} \\ &= w_k[0] + w_k[1]\end{aligned} \tag{16}$$

$$\begin{aligned}\sin\theta_{k,0} - \theta_{k,1} &= -c_{k,0}s_{k,1} + s_{k,0}c_{k,1} \\ &= w_{M+k}[0] + w_{M+k}[1]\end{aligned} \tag{17}$$

$$\begin{aligned}&\theta_{k,0} - \theta_{k,1} \\ &= \text{atan2}(w_{M+k}[0] + w_{M+k}[1], w_k[0] + w_k[1])\end{aligned} \tag{18}$$

and

$$\begin{aligned}\cos\theta_{k,0} + \theta_{k,1} &= c_{k,0}c_{k,1} - s_{k,0}s_{k,1} \\ &= w_k[0] - w_k[1]\end{aligned} \tag{19}$$

$$\begin{aligned}\sin\theta_{k,0} + \theta_{k,1} &= c_{k,0}s_{k,1} + s_{k,0}c_{k,1} \\ &= -w_{M+k}[0] + w_{M+k}[1]\end{aligned} \tag{20}$$

$$\begin{aligned}&\theta_{k,0} + \theta_{k,1} \\ &= \text{atan2}(-w_{M+k}[0] + w_{M+k}[1], w_k[0] - w_k[1])\end{aligned} \tag{21}$$

Likewise, (16) – (21) can still be used to "fit" a set of angles as in the case where $m = 1$. The following expressions indicate how much $w[n]$ differs from PC. The larger they are, the more $w[n]$ differs from PC.

$$D_{k-} = |1-(w_{M+k}[0]+w_{M+k}[1])^2-(w_k[0]+w_k[1])^2| \tag{22}$$

$$D_{k+} = |1 - (-w_{M+k}[0] + w_{M+k}[1])^2 - (w_k[0] - w_k[1])^2| \tag{23}$$

Finally, in both cases, the design process is finished if an acceptable stopband attenuation is achieved. If not, one can either optimize the fitted angles $\theta_{k,l}$, or start over with a different window.

Actually the above design process can be carried out for an arbitrary lowpass filter $w[n]$ that do not have to satisfy PC. But $p_0[n]$ typically do not well mimic the frequency response of $w[n]$. This often implies that $p_0[n]$ has less stopband attenuation than $w[n]$, since the coefficients of $w[n]$ are modified to ensure PC. So it is desirable that w[n] be almost PC to begin with. (13), (22), and (23) tell how much $w[n]$ differs from PC.

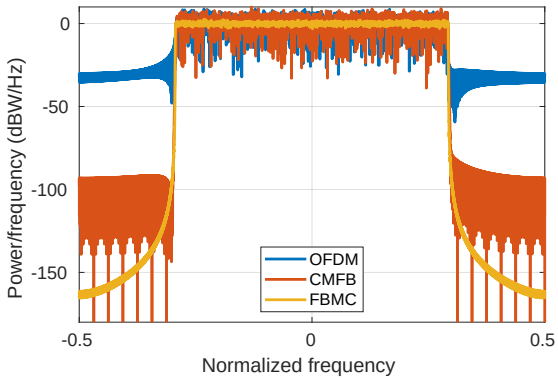

Figure 8: PSD comparison of three approaches: OFDM, FBMC and CMFB.

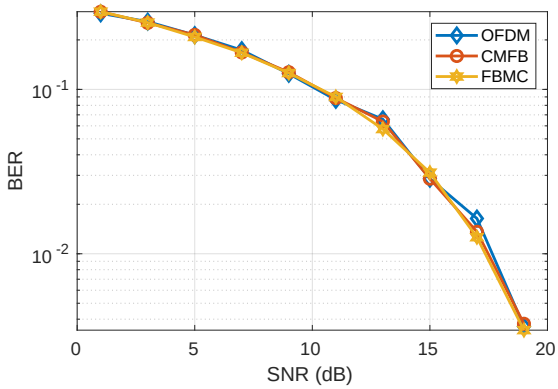

Figure 9: BER vs SNR for three approaches: OFDM, FBMC and CMFB.

FB and TMux are used interchangeably in this report, since both consist of an analysis bank and a synthesis bank. But [5] shows that a PR FB with no skew can be converted to a PR TMUX by interchanging the analysis and synthesis banks, and delay either bank of filters by 1. Alternatively, this delay can be incorporated into the channel, and simply swapping the analysis and synthesis banks of a PR FB would yield a PR TMux.

IV. Results

A. Methodology

We first design various prototype filters and analyse their magnitude response. Next we pick the best filter for FBMC and CMFB system and analyse the performance of communication system in terms of power spectral density (PSD) and bit error rate (BER). The PSD will give us an idea of how significant is the side-lobe leakage that affects nearby symbols in frequency domain. The BER tells us if the bits loaded in the sub carriers can be decoded correctly and verifies near perfect reconstruction is possible under the impact of noise.

In simulation, we generate random bits at the transmitter, modulate it with 64 QAM modulation and pass them as input to the synthesizer filter bank. We also process the complex modulated symbols and make them real by OQAM processing. The transmitted symbol is then passed through wireless channel. The wireless channel is modeled as AWGN

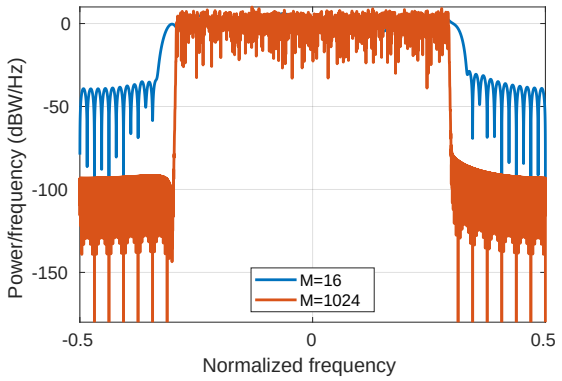

Figure 10: Effect on number of channels M

with noise power depends on the target SNR. Finally, the receiver implements the channelizer and reverse processing to recover the transmitted bits. We plot BER-SNR curve to analyse the performance of our multi-carrier system[1].

B. Comparison of OFDM, FBMC, and CMFB

First we plot PSD of OFDM, FBMC, and CMFB system in Figure 8. The average power is normalized for the three system. We observe that OFDM suffers from worse side-lobe leakage of around -30 dBW/Hz, followed by CMFB (-100 dBW/Hz). FBMC gives the best performance with side-lobe leakage less than -150 dBW/Hz. This makes FBMC the best choice for multi-carrier communication, however, with a tradeoff of higher complexity compared to OFDM.

Next, in Figure 9, we show BER vs SNR plots. We observe the performance of OFDM, FBMC, and CMFB system is almost same. We conclude that even though FBMC is not PR, it is not limited by NPR property, but dominated by the impact of noise which makes perfect reconstruction impossible for all the system. We note here that the performance of the three systems differs from the perspective of side-lobe leakage which affects the system when there are multiple users using adjacent frequency bands for communication. However, for a single user system that we have implemented, the BER performance is not affected. Also, note that for FBMC and CMFB system the filter spans a over multiple symbols, which we have accounted for by transmitting multiple symbols by overlapping them appropriately in time.

C. Effect on number of channels M

We see in Figure 10 that the PSD has much lower side-band leakage for larger M. Thus a larger M is preferred. However, large M will incur higher delay in obtaining the symbol as the receiver has to receive all M data points before it starts processing that symbol.

1) Effect of window functions: We compare the magnitude response of multiple filters for CMFB system as shown Figure 14. The observation here is that Kaiser window suits the best for minimizing side-lobe leakage. Other filters such as blackman window or blackman harris window has magnitude

[1]Our matlab code is available online at https://github.com/ishjain/ECE251C/

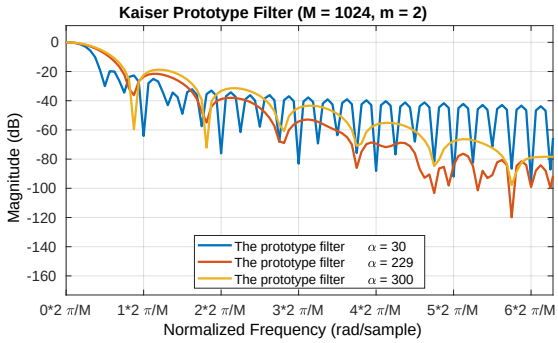

Figure 11: Effect Kaiser prototype filter parameter α

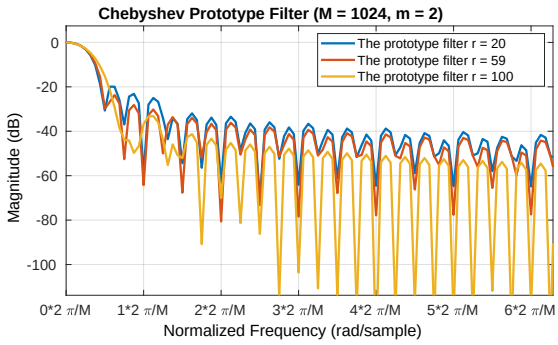

Figure 12: Effect Chebyshev prototype filter parameter r

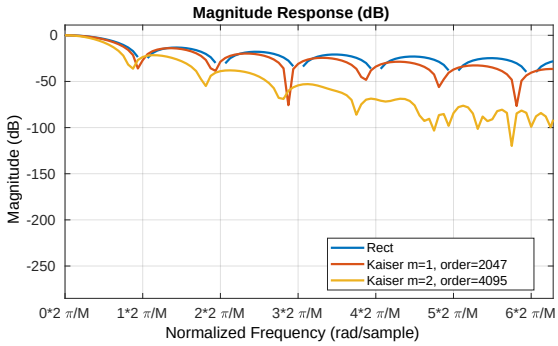

Figure 13: Effect Kaiser prototype filter order.

response better than rect window but worse compared to Kaiser window.

D. Effect of filter parameters for CMFB

1) Effect Kaiser prototype filter parameter α : As we see in Figure 11, a large α leads to lower side-band attenuation for far-away bands however at the expense of higher attenuation at the adjacent bands.

2) Effect kaiser prototype filter order : The Kaiser prototype filter with only a single stage ($m = 1$) does not give much advantage over rectangular window as shown in Figure 13. Using a higher order filter gives better performance in terms of reducing side-lobe leakage, however, with a tradeoff of higher implementation complexity.

3) Effect Chebyshev prototype filter parameter r : We observe in Figure 12 that the Chebyshev filter with $r = 100$ gives the minumum side-lobe leakage.

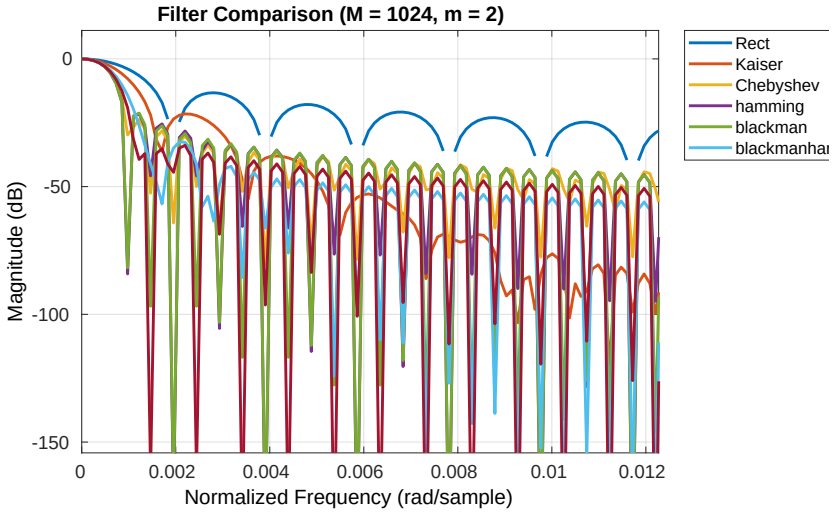

Figure 14: Comparison of prototype filter based on different windows.

APPENDIX

The "reverse engineering" design approach described in Section III is illustrated with some examples for a 16-channel CMFB ($M = 16$).

(1) $m = 1$

The length of $w[n]$ is hence 32 ($N = 31$). Note that only half of the coefficients are needed because of symmetry ($w[n] = w[N-n]$). Here the Hamming, Chebyshev, and Kaiser windows are considered. The coefficients are normalized such that $D_0 = 0$.

(i) Hamming

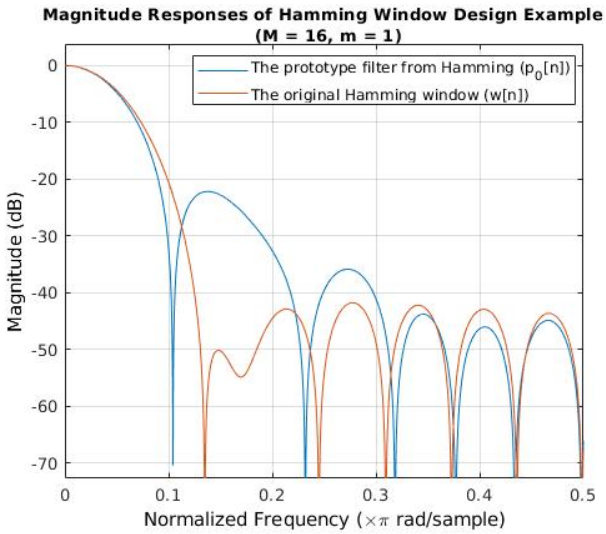

Figure 15: Comparison of magnitude responses for Hamming

(ii) Chebyshev

k	0	1	2	3
$w_k[0]$	0.0799	0.0893	0.1172	0.1623
$w_{M+k}[0]$	0.9968	0.9781	0.9414	0.8883
$\theta_{k,0}$ (rad)	1.4908	1.4797	1.4470	1.3901
D_k	0	0.0354	0.1000	0.1846
k	4	5	6	7
$w_k[0]$	0.2229	0.2964	0.3799	0.4699
$w_{M+k}[0]$	0.8209	0.7420	0.6547	0.5628
$\theta_{k,0}$ (rad)	1.3057	1.1907	1.0450	0.8751
D_k	0.2765	0.3616	0.4270	0.4624

Table I: A Hamming window example ($m = 1$ and $M = 16$)

k	0	1	2	3
$w_k[0]$	0.4057	0.2224	0.2774	0.3367
$w_{M+k}[0]$	0.9140	0.9036	0.8830	0.8528
$\theta_{k,0}$ (rad)	1.1530	1.3295	1.2663	1.1948
D_k	0	0.1341	0.1434	0.1594
k	4	5	6	7
$w_k[0]$	0.3992	0.4636	0.5288	0.5932
$w_{M+k}[0]$	0.8138	0.7671	0.7138	0.6553
$\theta_{k,0}$ (rad)	1.1148	1.0271	0.9332	0.8352
D_k	0.1784	0.1967	0.2109	0.2187

Table II: A Chebyshev window example ($m = 1$, $M = 16$, and $r = 30$)

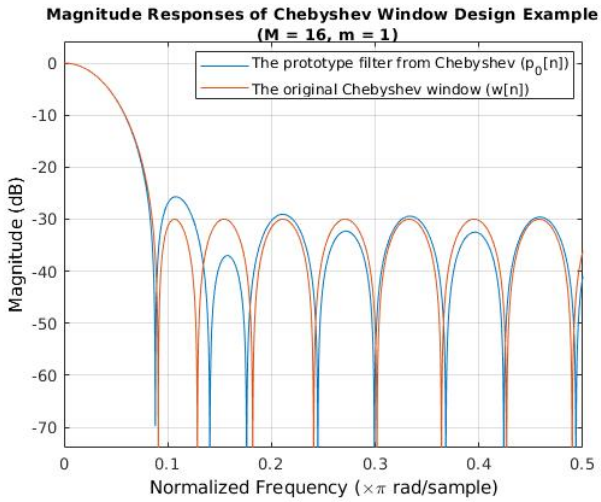

Figure 16: Comparison of magnitude responses for Chebyshev

(iii) Kaiser

k	0	1	2	3
$w_k[0]$	0.3748	0.4291	0.4832	0.5366
$w_{M+k}[0]$	0.9271	0.9213	0.9097	0.8924
$\theta_{k,0}$ (rad)	1.1866	1.1349	1.0825	1.0294
D_k	0	0.0328	0.0610	0.0843
k	4	5	6	7
$w_k[0]$	0.5886	0.6388	0.6864	0.7311
$w_{M+k}[0]$	0.8698	0.8419	0.8093	0.7722
$\theta_{k,0}$ (rad)	0.9758	0.9218	0.8673	0.8127
D_k	0.1030	0.1169	0.1261	0.1308

Table III: A Kaiser window example ($m = 1$, $M = 16$, and $\alpha = 30$)

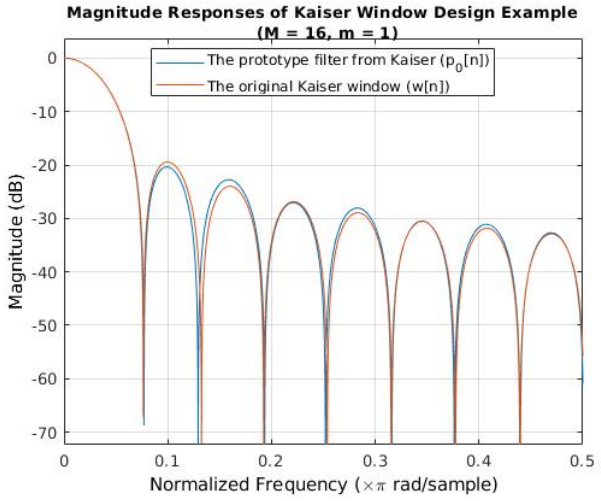

Figure 17: Comparison of magnitude responses for Kaiser

As is illustrated above, the larger the D_k, the more different $p_0[n]$ and $w[n]$ are, which typically means the worse the sidelobe attenuation. In the Hamming window example, the largest sidelobe grows by almost 20 dB. The largest sidelobe in the Chebyshev example only grows by around 3 dB. The magnitude responses of $p_0[n]$ in the Kaiser window example is almost the same as $w[n]$.

REFERENCES

[1] G. Strang and T. Nguyen, *Wavelets and filter banks*. SIAM, 1996.

[2] M. Bellanger, "Digital signal processing. theory and practice," 1985.

[3] A. Viholainen, M. Bellanger, M. Huchard *et al.*, "Phydyas project, deliverable 5.1: Prototype filter and structure optimization," *FP7-ICT, Tech. Rep*, 2009.

[4] P. P. Vaidyanathan, *Multirate Systems and Filter Banks*. Englewood Cliffs: Prentice Hall, 1993.

[5] R. D. Koilpillai, T. Q. Nguyen, and P. P. Vaidyanathan, "Some results in the theory of crosstalk-free transmultiplexers," *IEEE Trans. Signal Processing*, vol. 39, no. 10, pp. 2174–2183, Oct. 1991.